Reduction of the hot cracking sensitivity of CM-247LC superalloy processed by laser cladding using induction preheating

Guillaume Bidron, Anis Doghri, Thierry Malot, Florent Fournier-Dit-Chabert, Marc Thomas, Patrice Peyre

Reduction of the hot cracking sensitivity of CM-247LC superalloy processed by laser cladding using induction preheating

G. Bidron[1,4], A. Doghri[2,3], T. Malot[1], F. Fournier-dit-Chabert[2], M. Thomas[2] and P. Peyre[1]

[1] Laboratoire PIMM, UMR 8006 CNRS - Arts et Métiers ParisTech – CNAM, 151 Bd de l'Hôpital, 75013, Paris, France

[2] ONERA - The French Aerospace Lab., 29 Avenue de la Division Leclerc, 92322 Chatillon Cedex, France

[3] Université de Lorraine, CNRS, Arts et Métiers ParisTech, LEM3, F-57000 Metz, France

[4] APS Coatings, Rue de la Mare Blanche, 77186 Noisiel, France

Abstract

In the present work, the repair of CM-247LC superalloy has been investigated by using a laser cladding process. Since this material is well known for its high hot-cracking susceptibility in Heat Affected Zone during welding, repairing is quite challenging. In a first stage, a detailed investigation of the effect of cladding parameters on the crack susceptibility was carried out on coupons that received a low pre-heating condition. However, despite a reduction of crack sensitivity for low energy inputs, this material has systematically shown some evidence of cracking in the HAZ. In a second stage, attempts were made to reduce crack defects by using an induction preheating, with higher temperatures in the range of 800 - 1100°C. With the highest pre-heating temperatures near 1100°C, the partial dissolution of large γ' precipitates, combined with re-precipitation of secondary and smaller γ' precipitates were helpful to prevent hot cracking.

Keywords: cladding, laser, CM-247LC, preheating

1. Introduction

Nowadays, a high number of aeronautical parts are produced by the casting route. Depending on the casting conditions and the chemical composition, some parts can present detrimental defects which lead to their non-acceptance. In many aspects (cost, environment …), a refurnishing step appears to be an attractive solution for ensuring a second life to mechanical parts at an affordable cost. However, if most of metallic parts can be repaired by existing processes (arc or laser melting for instance), a number of materials cannot easily be repaired, mainly due to their hot or cold cracking sensitivity.

The present work is focused on the homogeneous repairing of CM-247LC parts, a nickel-based superalloy implemented in hot sections of gas turbine engines. This alloy exhibits high strength at elevated temperature, combined with a good hot corrosion resistance.

This alloy is strengthened by precipitation of the γ' phase, $Ni_3(Al,Ti)$, which is homogeneously distributed in the γ matrix. Due to its high Al and Ti content, resulting in a high γ' ratio (approximately 60-65 %), and according to Lippold (2011), such high γ' superalloys are commonly considered as very

difficult to weld due to its high cracking susceptibility in the Heat Affected Zone (HAZ) during welding together with strain age-assisted cracking during post weld heat treatment. For instance, such a specific behavior of high γ' alloys is reported by Ojo (2004) on Inconel 738. In the meantime, on similar alloys, a nil-ductility is mentioned in the patent from Smashey (2009), on a 400°C range below the solidus, resulting in an enhanced cracking susceptibility.

In his early work, Owczarski (1966) reported that liquation of grain boundaries was the primary cause of low HAZ crack resistance in most austenitic alloys. As a non-equilibrium reaction, liquation leads to local melting within grain boundaries, at a temperature below the alloy's solidus. This eutectic-type reaction occurs between a second phase particle (γ', carbide …) and the matrix, thus leading to the formation of a non-equilibrium solute rich film at the particle/matrix interface as shown by Ojo, (2004). Therefore, the material can be teared apart during solidification and cooling due to the presence of a liquid phase. A number of causes are known to promote the liquation phenomenon:

- Ernst (1987) indicated that Nb and Ti increase the crack susceptibility of fully austenitic alloys (like CM247LC)
- Ojo (2004) mentioned that Al and Ti are melting point depressants, increasing the risk of local melting point and that MC carbides, borides, eutectic and coarse γ' precipitates are strong contributors to the HAZ liquation cracking.
- Danis (2010) confirmed that larger γ' precipitates are more deleterious on In738 alloy than smaller ones because with large γ' promote liquation whereas a fine precipitation decreases the risk of liquation, but significantly increases the crack sensitivity during post-welding heat treatment.

The preheating and post-heating stage is usually recommended by the welding community to limit thermal gradients G (K/m) during cooling, thus improving their resistance to hot tearing. However, hot cracking is also directly dependent on γ' precipitate rate. Materials with more than 50-55 % of γ' are commonly known as difficult to weld. However, there is still a need to establish a precise and universal correlation between γ' content, γ' size and hot-cracking sensitivity. In a classical weldability map representing weldable and non-weldable zones as a function of Ti and Al contents, CM-247LC (also known as MARM-247 alloy) is considered as very sensitive to hot cracking, due to its high Al and Ti contents (> 6.0 wt.%).

Various patents have been reported for the welding repair of high γ' nickel-based superalloys with high cracking susceptibility and nil-ductility temperature range, with the use of optimized pre and post-heating stages. Among those patented works:

- Smashey, (1999) proposed a three step procedure for welding materials having nil-ductility range between the solidus temperature and 400°C below the solidus temperature (R108, René80, Mar-M247, Mar-M200) involving: (1) matter removal followed by high temperature stress relief, (2) arc welding-repairing at a given pre-heating welding temperature of 1000-1150 °C and (3) a second stress relief.
- Foster (2001) patented a repair procedure under controlled atmosphere with the use of a high induction preheating and post-heating temperature to allow a maximum ductility temperature range for Inconel 738 like alloys, followed by an optimized two-step cooling (a rather fast argon fast quenching to an intermediate temperature, then a slower one) to limit γ' precipitation.
- Morin (2009) proposed a welding solution at ambient temperature for hot-cracking sensitive superalloys, without preheating, but with incorporation of a ductile filler material like Hastelloy W or Inconel 625 allowing a mitigation of thermally induced stresses. For the

specific case of CM247LC, this patent includes a pre-welding heat-treatment procedure to limit γ' percentage to 40-55 %

Danis (2010) confirmed the benefit of an optimum preheating stage at high temperature for the GTAW repairing of IN738LC, another high γ' precipitation-strengthened superalloy.

Globally, there is a lack of published data related to welding, fusion defects or repairing on CM247LC (or Mar-M 247). In his PhD work, Mc Nutt (2015) carried out laser cladding experiments of CM247LC for repair applications but could not fully suppress welding cracks, even when pre-heating at 800°C. Hagedorn (2013) obtained successful results on CM247LC specimens using powder bed fusion (SLM). Similarly, Basak (2017) has shown that the Scanning Laser Epitaxy technique could allow repairing Mar-M247 parts on a large thickness with a single pass. Last, successful dissimilar laser butt-weld joints between Hastelloy X and Mar-M 247, were demonstrated by Li (1997), using deliberate misalignments of the laser heating on Hastelloy to suppress cracking.
In the present work, some preliminary process and microstructural investigations are presented, involving different preheating stages in the 400°C – 1100°C temperature range coupled with different laser energy inputs. The objective was to define adequate process conditions for avoiding cracks during repair of the CM247LC parts for aeronautical applications.

2. Experimental procedure

As-received CM-247LC part was provided by Arconic as a large cast stator heat shield (Figure 1). Standard treatment includes a 4-hour hot isostatic pressing at 1185°C followed by a two-step heat treatment (1232°C for 2 hours followed by 1080°C for 2 hours) and then gas cooling. From this large part, two types of samples were extracted: from the upper "plateau" part (type 1) and from the bottom "feet" part (type 2). Extracted samples consisted of 4 x 3 x 2 mm and 4 x 3 x 4 mm plane coupons.

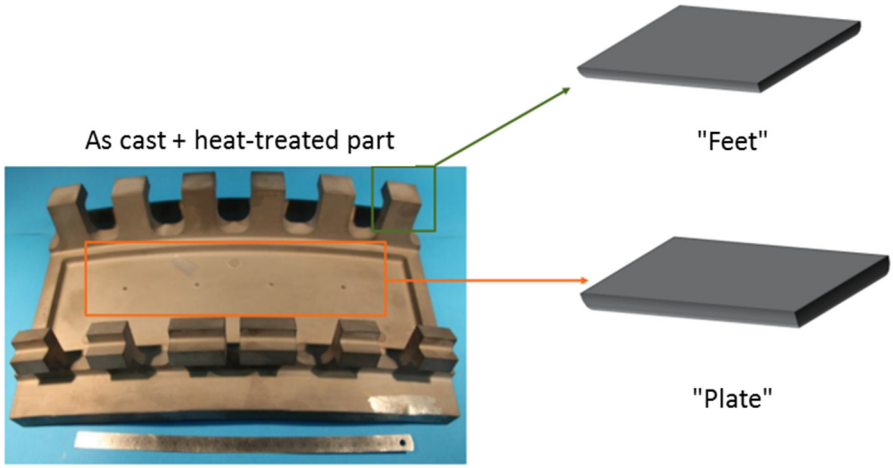

Figure 1: As-received stator heat shield + heat treated part from which type 1 and type 2 coupons are extracted. Coupons thicknesses are either 2 or 4 mm.

CM-247LC powder was gas-atomized (VIGA atomization set-up) at Onera starting from ingots provided by Arconic. Its chemical composition in weight percent is given in table 1.

	Ni	Co	W	Cr	Al	Ta	Ti	Mo	Hf	C
Substrate	Bal	9.4	9.5	8.47	5.55	3.2	0.74	0.46	1.5	0.08
Powder	Bal	9.4	9.2	8.1	5	3	0.9	0.5	1.3	0.05

Table 1: Nominal weight percent composition of CM247LC powder and substrate

Metallographic expertise of the powders did show that some powder particles exhibit internal porosities and some others were not fully spherical (Figure 2). Anyway, the flowability of the powder was sufficient for ensuring stable powder feeding during the cladding experiments. The powder size distribution was in-between 25 µm and 120 µm, with a D_{50} diameter of 70 µm.

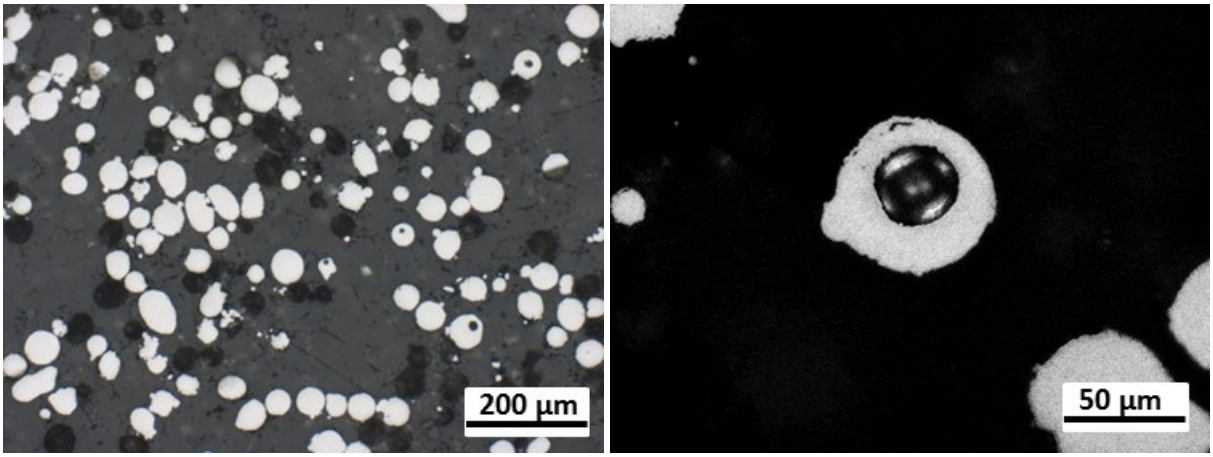

Figure 2: Optical micrograph of CM247LC powders at (a) low magnification and (b) higher magnification, with occluded porosity in a powder grain.

The experimental deposition tests were carried out mostly using an OPTOMEC system equipped with a 3 kW Nd: YAG TRUMPF laser operating at 1.06 µm, and some additional tests have been carried out using a 10 kW Yb:YAG TRUMPF laser operating at 1.07 µm wavelength. An helicoïdal coaxial nozzle was used to deliver the powder. The corresponding powder stream has a 2.5 mm diameter at focus point, where it interacts with the laser-induced melt-pool. The powder capture efficiency is between 60 % and 80 %, depending on the melt-pool width. In this study, low mass feed rates were used (1 to 2 g/min) as repaired area did not require thick cladding layers. The operating parameters are listed in Table 2.

Nozzle type	Coaxial
Work distance (mm)	10 to 20
Spot size D (mm)	2 to 4.6
Scanning speed V (mm/min)	25 to 400
Power P (W)	100 to 1500
Mass feed rate D_m (g/min)	1 to 2
Powder stream diameter D_p (mm)	2.5
Preheating (°C)	400 – 1100°C

Table 2: Main operating parameters conditions used for CM247LC laser cladding

As many process parameters were used, an energy density parameter called fluence (F) was proposed to combine the different process parameters in a single one. This F parameter was calculated by multiplying the power density $P/(\pi D^2/4)$ by the maximum interaction time (D/V) of the laser with the substrate.

For every test, the substrates were first preheated by means of a 25 kW magnetic inductor from CEIA Company, and the temperature was controlled via a type K thermocouple located near the cladded area (Figure 3). Clad repairs have been performed without global shielding of the part, i.e. just with carrying gas (Ar). Considering previous studies by Gharbi (2012) on the same device, the local O_2 ratio was estimated to be comprised between 1000 and 2000 ppm. The present work aims at defining a weld crack-free procedure, in terms of pre-heating temperature and laser repair parameters, starting with single fusion beads before performing overlapped beams to repair larger areas.

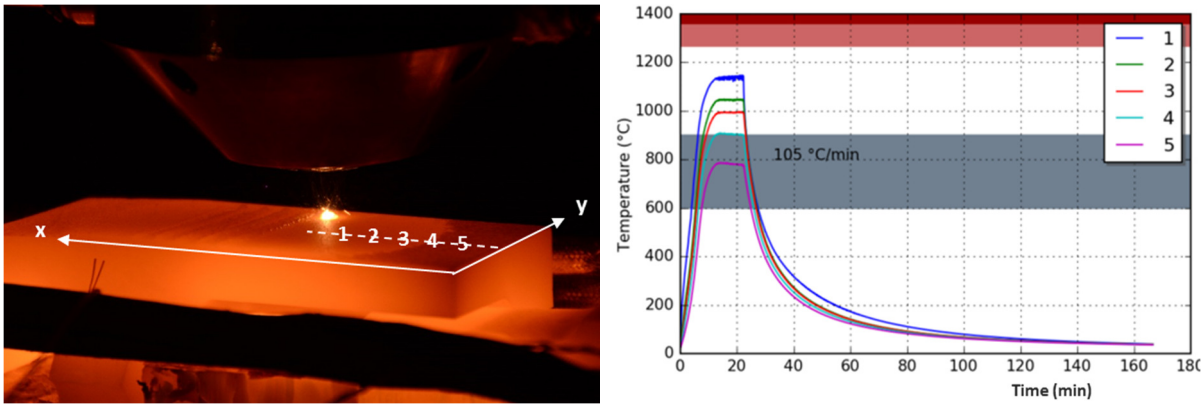

Figure 3: Laser cladding using induction heating. (a) Picture of the running process on a 100 x 25 x 15 mm sample (b) Typical heat-cycles recorded by the thermocouples positioned on various locations at the surface of the sample (with 1 to 5 as follows: 1 (30 mm, 12.5 mm), 2 (25,12.5), 3 (20,12.5), 4 (15, 12.5), 5 (10, 12.5)) for a 10 minutes temperature plateau.

Subsequent samples have been cross sectioned, polished both mechanically and with diamond paste and then etched electrolytically (12 mL H_3PO_4, 40 mL HNO_3, 48 mL H_2SO_4 at 6 V during 5 s). Microstructures were examined by optical microscopy and by using a Zeiss scanning electron microscope (SEM).

3. Results

3.1 Microstructure of pre-weld heat treated specimens

Solution heat-treated CM247LC samples exhibit a dendritic structure with heterogeneous γ' precipitation (65 % estimated γ' content). Dendritic cores are prone to form finer submicron cuboid precipitates (≈ 400 nm) whereas inter-dendritic regions exhibit a more complex microstructure consisting of γ - γ' eutectics, coarser precipitates and carbides (Figure 4).

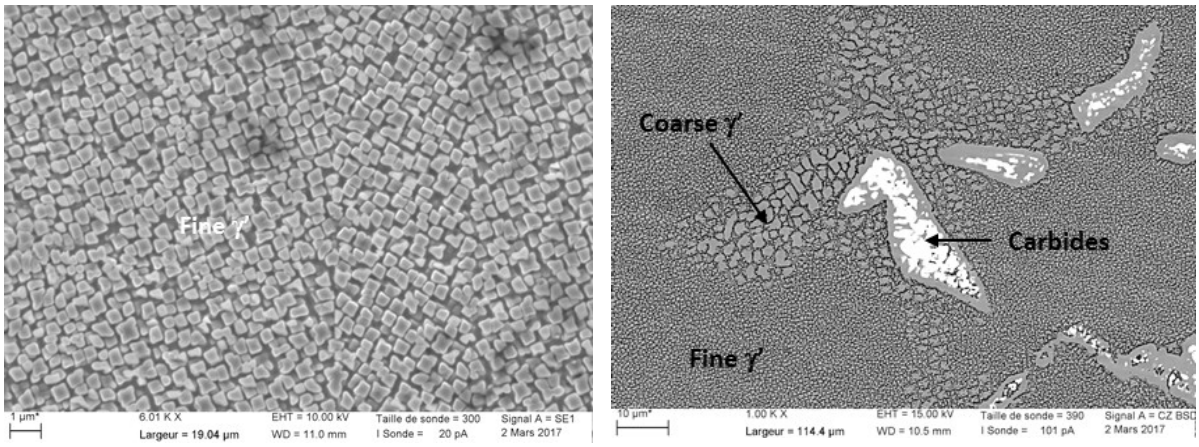

Figure 4: Microstructure of as received CM247LC substrates (a) Fine γ precipitates (≈ 60-65 % γ) in γ dendrites, (b) Inter-dendritic zones with (Ti, Al, Hf) C carbides and coarse γ

3.2 Morphologies and Microstructures of single beads obtained without preheating and with a low (400°C) preheating temperature

In a first step, single beads were analyzed to optimize their shape, and to detect the occurrence of cracks in solidified materials. Preliminary trials have been made at room temperature without preheating (Figure 5), but have shown systematic hot cracking in the heat affected zones below and at the lateral side of beads, whatever the process conditions.

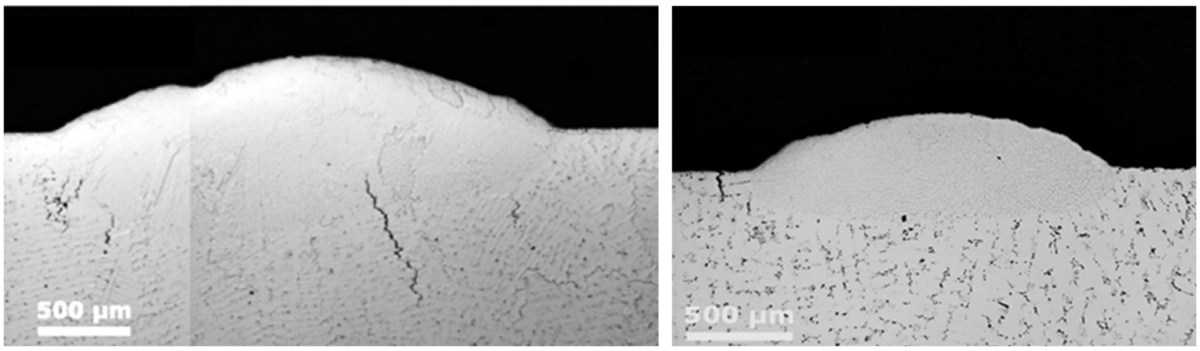

Figure 5: Examples of single fusion beads obtained without preheating on CM 247LC for two distinct laser diameters. (a) D = 4.6 mm, P= 1000 W, V = 100 mm/min (b) D= 2 mm, P = 700 W, V = 100 mm/min

In a second step, a low preheating temperature was used. Figure 6 shows cross sections of single beads carried out for two scanning speeds (50 and 100 mm/min) and four laser powers (100, 200, 320, 400 W) with a preheating temperature of 400°C. A near-half-spherical shape is commonly observed for every bead, with heights of 0.4 to 1.4 mm, dilution rates (= ratio of molten substrate volume over total molten volume) of 5 % to 60 % and wetting angles α in the range of 25° to 100° depending on the operating conditions. Logically, lower heights and better wetting are obtained at high power. Even at low magnification, macrocracks are evidenced at P=1000 W, whereas beads are apparently sound at lower powers.

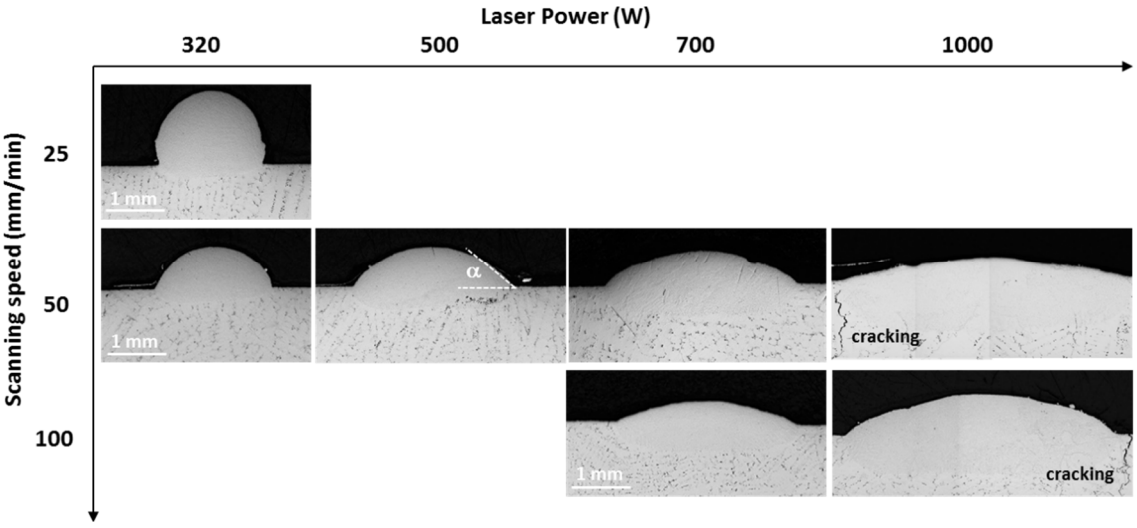

Figure 6: Macroscopic analysis of single fusion beads for various laser powers and scanning speeds. Below macrographs are reported dilution rate values (= ratio of molten volumes $V_{substrate}/V_{total}$) - Preheating temperature = 400°C, D = 2 mm

The different parts of a single bead, evidenced with a chemical etching (Figure 6), can be described as follows:

- The molten or Fusion Zone (FZ) is composed of equiaxed dendrites corresponding to the fastest cooling rates in the upper zone, and just below of columnar dendrites oriented in the direction of maximal thermal gradient G (K/m).
- A dilution zone, where the filler metal (in the present case, the powder) is mixed with the molten substrate metal.
- A Heat Affected Zone (HAZ) in the substrate where the material is subjected to metallurgical transformations ergo, a partial dissolution of γ' precipitates.
- Below the HAZ, no alteration of the initial microstructure is found which is referred as Base Metal (BM).
- The boundary between HAZ and mixed area clearly appears whereas the border between HAZ and the non-affected material is not so easy to point out. For the specific condition of Figure 7 (0.25 GJ/m²), a liquation open crack is evidenced in the lateral HAZ.

In Figure 8, the evolution of the microstructure along a crack located in the HAZ below the FZ (Figure 8a) is shown in more details:

- The crack initiates in the HAZ, just below the FZ limit, and propagates in near-eutectic interdendritic zones at the interface between large (Ti,C,Hf) carbides and coarse γ' precipitates (Figure 8 b,c)
- In near-eutectic zones, a crowned halo can be observed surrounding γ' precipitates and carbides. This halo indicates that a liquid film is formed around carbides and γ' (Figure 8d). This phenomenon, known as liquation in the literature (Ojo, 2004), is very common in small eutectic areas where low fusion temperature zones are re-melted, eventually leading to liquid pockets flowing within grain boundaries which have a very low mechanical resistance during cooling and therefore are prone to tearing

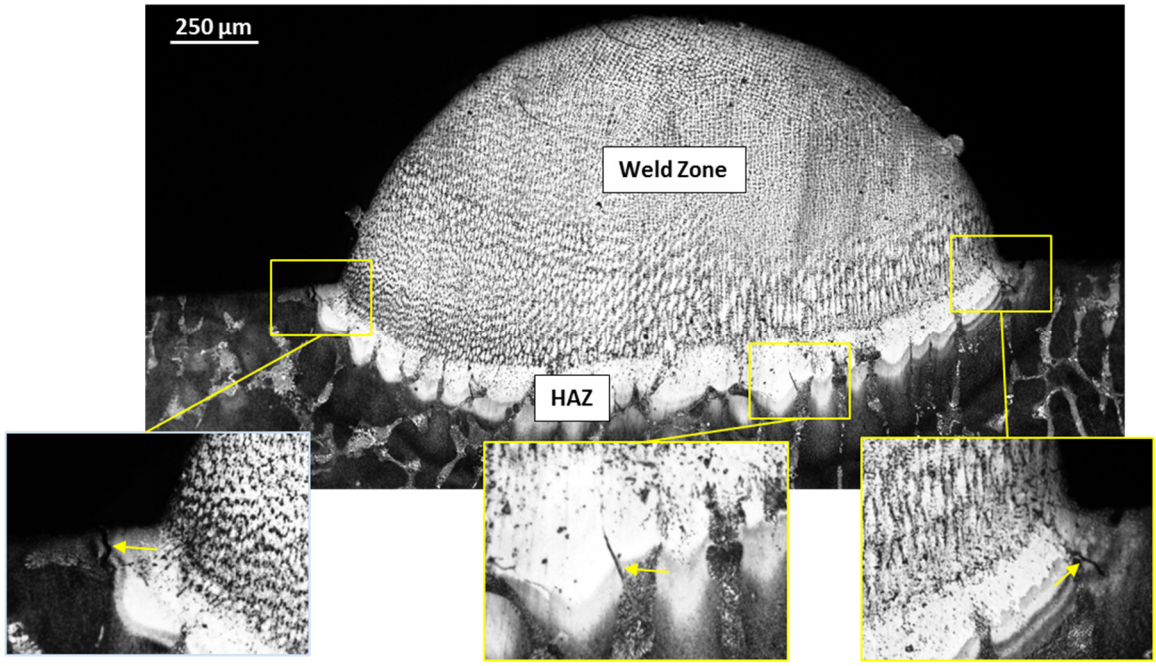

Figure 7: Metallographic cross section of a CM247LC single deposit (320 W – 50 mm/min – D= 2 mm, preheating temperature: 400°C) after chemical etching with 3 zooms on liquation cracks in HAZ

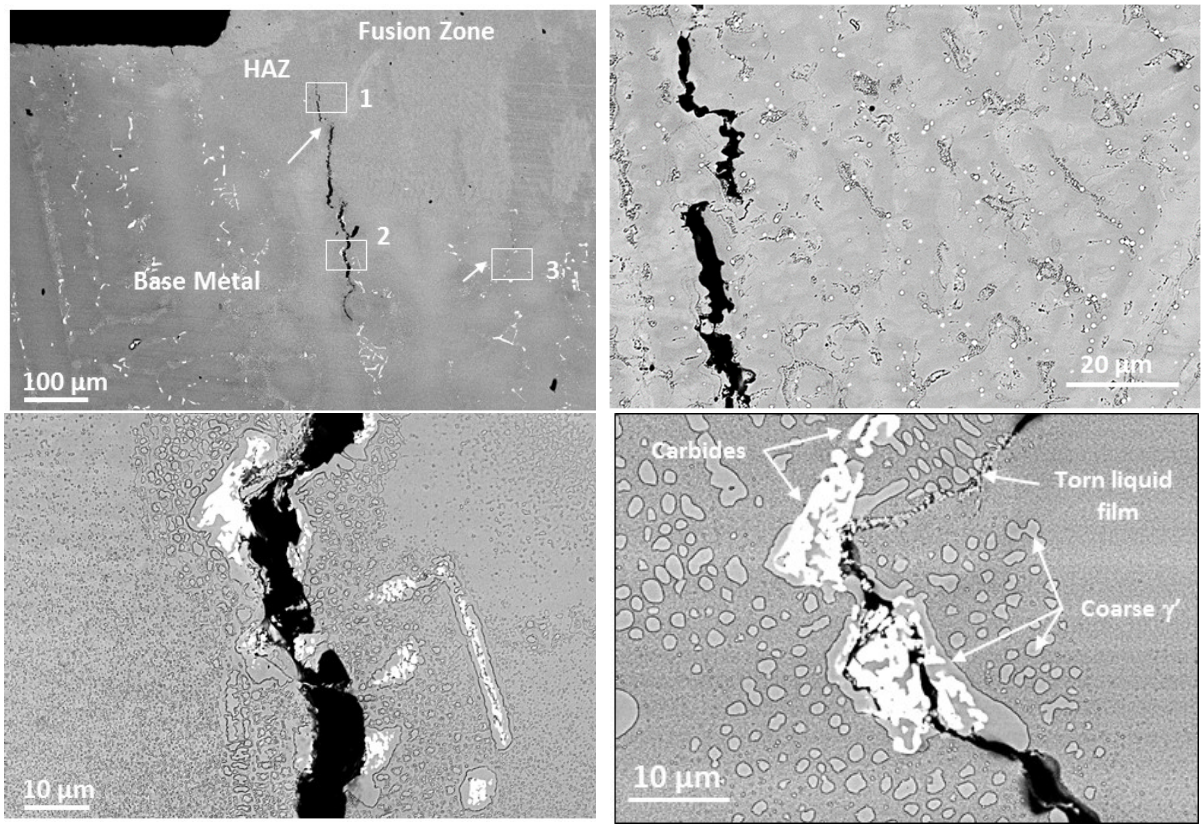

Figure 8: SEM analysis of hot cracking in the heat-affected zone, (a) at low magnification with windows 1, 2, 3, (b) detail of zone 1 near the crack initiation, (c) detail of zone 2, (d) detail of zone 3 with a small crack in an interdendritic zone (P=320 W – V=25 mm/min – D= 2 mm)

3.3 Influence of process parameters on the crack sensitivity of single beads

An estimation of the crack sensitivity can be easily obtained by determining crack lengths from micrographs, followed by image analysis. For this purpose, clad coupons have been cut in three sections to observe at least three locations so as to provide a reliable statistical approach. When no crack is observed, samples are systematically polished again to confirm the absence of crack occurrence. As the number of metallographic cross section varies from one condition to one another, the crack length measured is divided by the number of cross sections, giving a mean crack length per cross section of single beads.

Some attempts have been made to correlate average crack lengths with process parameters in terms of laser power, scanning speed, laser diameter and for different pre-heating temperatures (400°C, 750°C, 1050°C). The energy density parameter F combining P, V and D has also been tested as a possible indicator of crack sensitivity. Figure 9 presents the evolution of the crack sensitivity with the laser fluence F (J/m²) for respectively 2 mm and 4.5 mm spot diameters, and a preheating temperature of 400°C. From this Figure, we can draw the following conclusions:

- No crack-free bead could be obtained with a preheating as low as 400°C. Cracks are systematically observed in HAZ, and more randomly in the fusion zone (FZ);
- Low power and low scanning speed (i.e. low fluence) tend to reduce the crack sensitivity.
- The laser fluence (or energy density) cannot be considered as a fully adequate criterion to measure the crack sensitivity even if cracking mostly increases for higher F values. For instance, in Figure 9b, two conditions can be compared with a similar fluence of 0.23 GJ/m². The first one is carried out with a high power and a large diameter (700 W, D=4.5 mm), and the second with a lower laser power and smaller diameter (320 W, D=2 mm). It then appears that the 1st condition generates 7 times more crack lengths than condition 2.
- Crack length is minimized for the smaller (2 mm) diameter (Figure 9). Moreover, for a 2 mm spot diameter, cracks are always observed in the upper part of the substrate (visible for the outside), whereas for a 4.5 mm spot diameter, cracks are mainly located below the single bead.

Similar results were obtained for cladding tests performed at room temperature.

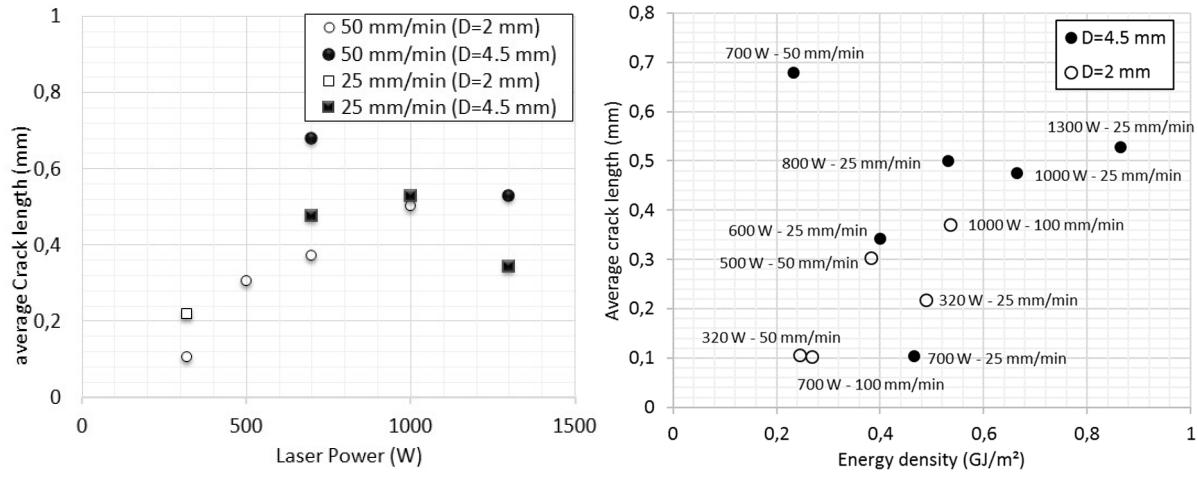

Figure 9: Average crack length versus laser power and energy density for a 400°C preheating and two laser spot diameters (2 and 4.5 mm).

Additional tests were carried out with a pre-heating temperature of 750°C and a 2 mm spot diameter (Figure 10). Surprisingly, using a pre-heat at 750°C induced a significant increase in crack susceptibility, together with a reduction of wetting angle.

This intensification of hot cracking at 750°C might be explained by the ductility dip phenomenon occurring in the 600-900°C temperature range for CM247LC and already mentioned by Carter (2014) on SLM samples and Kim (2011) on wrought samples. This ductility dip (significant reduction of the elongation rate during tensile tests under quasi-static conditions) can be responsible for a high susceptibility to cracking during cooling of the beads. At temperatures above 900°C, the ductility is expected to be recovered.
To avoid this deleterious behavior, two combined strategies have been adopted:

- Increasing the preheating temperature over 900°C to avoid the ductility drop.
- Working at low laser fluence (less than 0.2 GJ/m²) by using lower powers combined to low scan speeds to further reduce the crack sensitivity.

The first single beads carried out with a pre-heating temperature of 1050°C have been shown to provide satisfactory crack-free microstructures. Following such encouraging results, beads' overlaps were performed to produce 3D deposits.

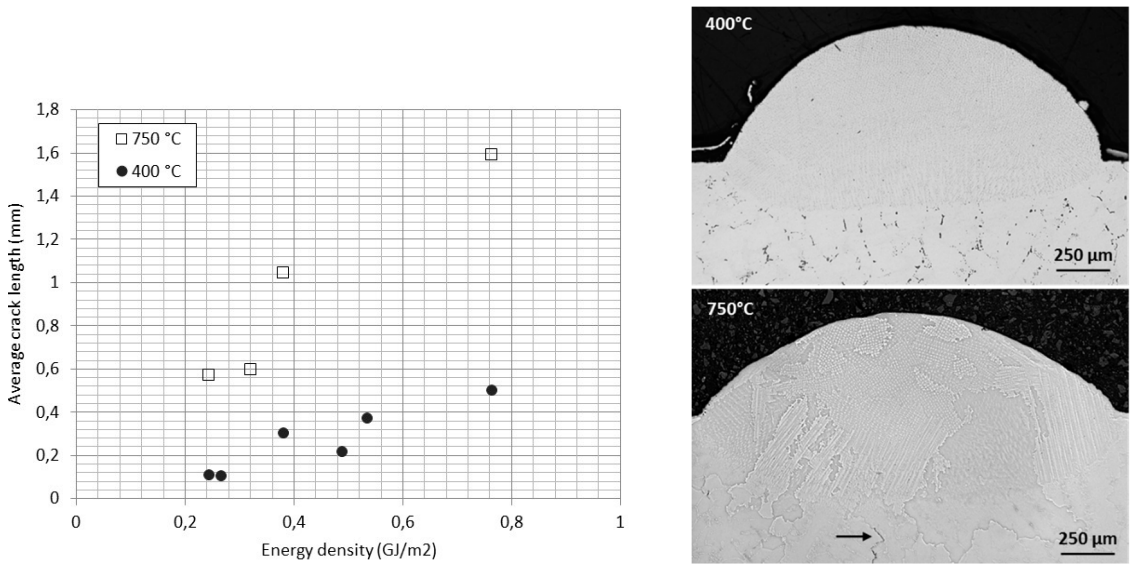

Figure 10: (a) Average crack length versus laser energy density for two distinct substrate preheating temperature (400 and 750°C), and a 2 mm spot diameter, (b) comparison of single beads obtained at 400°C and 750°C (320 W – 50 mm/min – D= 2 mm): a subsurface cracking is evidenced at 750°C

3.4 Microstructure of overlapped beads with high temperature preheating

Different samples have been cladded with a multi-bead configuration, with a pre-heating temperature of 1050°C and a reduced Fluence of 0.1 GJ/m² (150 W, 50 mm/min), on 2 different substrates: 4 mm-thick (sample 1) and 2 mm-thick (sample 2), both extracted from the initial stator (Figure 1):

1. In the first case (type 1 samples) the material deposit exhibits liquation cracks in the HAZ (Figure 11).
2. In the second case (type 2 samples) clad layers are crack-free. This result was confirmed on four different samples with four cross-sections on each sample, without observing any detectable crack (Figure 12).

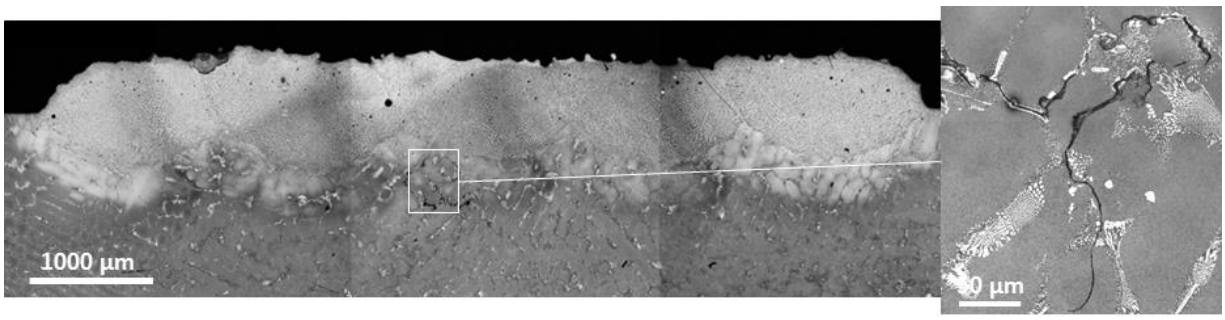

Figure 11*: Metallographic cross section observation of sample 1 (preheating temperature = 1050°C, 4 mm-thick, 150 W, 50 mm/min, D=2 mm): Liquation cracking in HAZ*

(a)

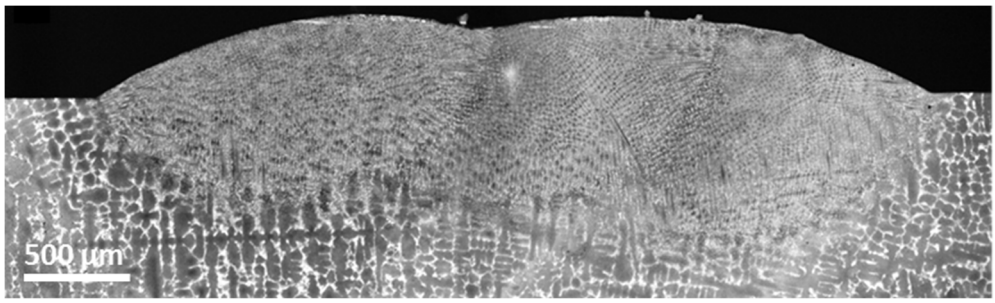

(b)

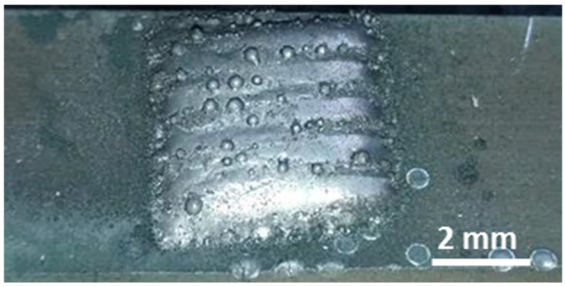

(c)

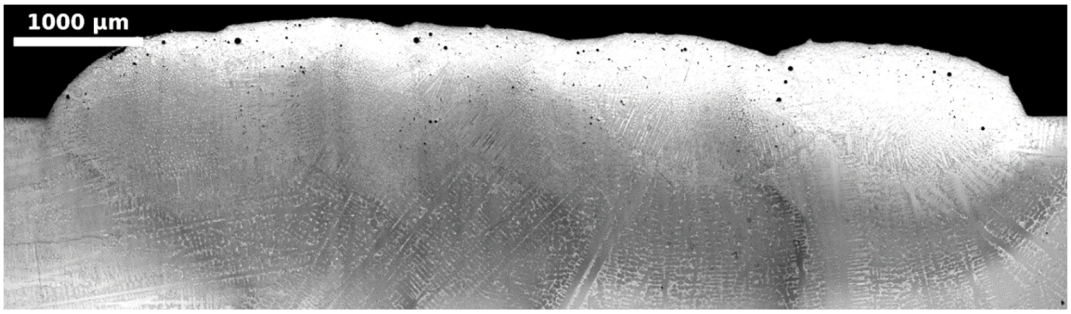

Figure 12: Analysis of crack-free samples (samples 2, 2 mm-thick, 150 W, 50 mm/min, D=2 mm) (a) metallographic analysis of 2 beads overlap (b) Macroscopic picture and (c) metallographic analysis of a 5 beads overlap (preheating temperature = 1050°C)

For both configurations, small (< 0.1 mm) spherical porosities (gas entrapping) are always observed in the deposit. A detailed analysis of sample 2 revealed a classical hot tearing of liquid films located in eutectic interdendritic zones, at the interface with large γ' precipitates (Figure 13).

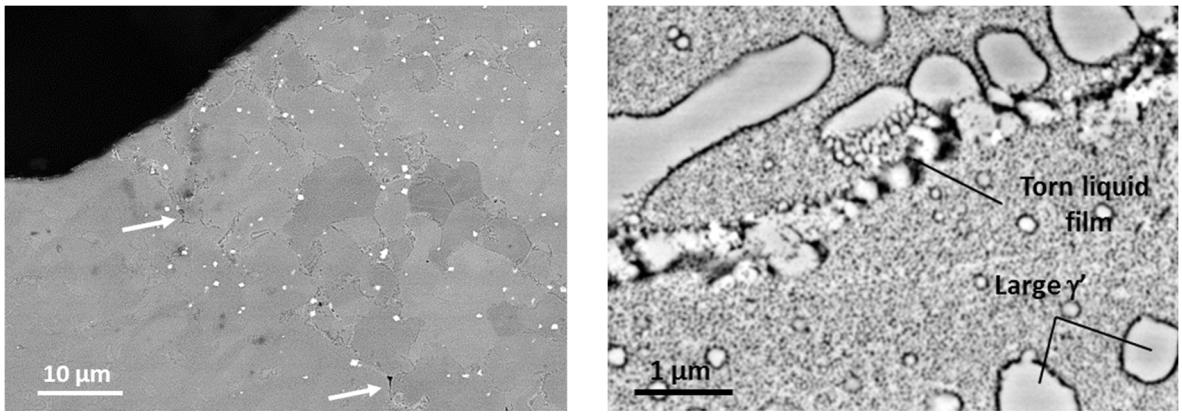

Figure 13: Detailed cross section of Sample 4 (4 mm-thick, 150 W – 50 mm/min): location of liquation cracks in the inter-dendritic zones near large γ' precipitates

4. Discussion

Results presented here above indicate that a repairing procedure is possible on CM-247LC (or Mar-M247) with temperature pre-heating of at least 1050°C. However, depending on substrate thickness, local cracking in HAZ is still possible.
The reason why samples 1 (thickness = 4 mm) and 2 (thickness = 2 mm) behaved in a different manner with similar processing parameters can be explained by different options:

1. A residual stress effect: during solidification and cooling, clad layers are submitted to tensile stresses generated by the surrounding matter, which are enhanced by thicker substrates
2. Modifications of local thermal cycles due to specific heat dissipation during induction heating which generate different microstructural effects, especially in terms of γ' content.

For a deeper understanding of microstructural effects, a detailed analysis of γ' precipitation was carried out. On the one hand, for 2 mm – thick crack-free samples (type 2 samples), the primary γ' content is shown to be very low (≈ 16 %) in the HAZ and just below the HAZ whereas a large amount of small (≈ 50 nm) γ' secondary precipitates are observed (Figure 14a). On the other hand, for 4 mm – thick samples, the microstructure in and just below the HAZ is fully composed of 55-60 % primary γ' precipitates (size ≈ 500 nm), which content is very similar to the one of initial substrates. Consequently, for similar applied induction heating, it is assumed that different local thermal cycles T=f(x,y,z,t) were really applied to the substrates.

To further address this point, isothermal heat treatments have been carried out, using time holding of 15 min, 30 min and 60 min at temperatures of 950°C, 1050°C and 1100°C, for 2 mm-thick substrates. Results indicate that a precipitate state equilibrium has occurred after only 15 min, and that dissolution of γ' tends to be effective only for T=1100°C and above (Figure 15). This confirms that, for similar durations as induction heating cycles, the dissolution of primary γ' precipitates is not really effective below 1100°C.

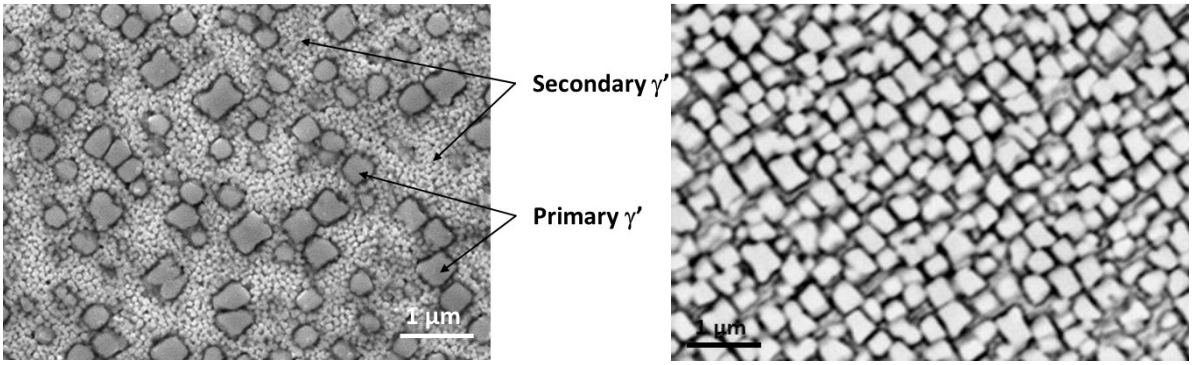

Figure 14: Microstructure of CM-247LC after induction HT at 1050°C on (a) 2 mm thick sample and (b) 4 mm-thick sample. On 2 mm-thick sample, the primary γ' content is near 16 % and tiny secondary γ' precipitates are formed whereas on 4 mm – thick samples the primary γ' content is still close to 60%.

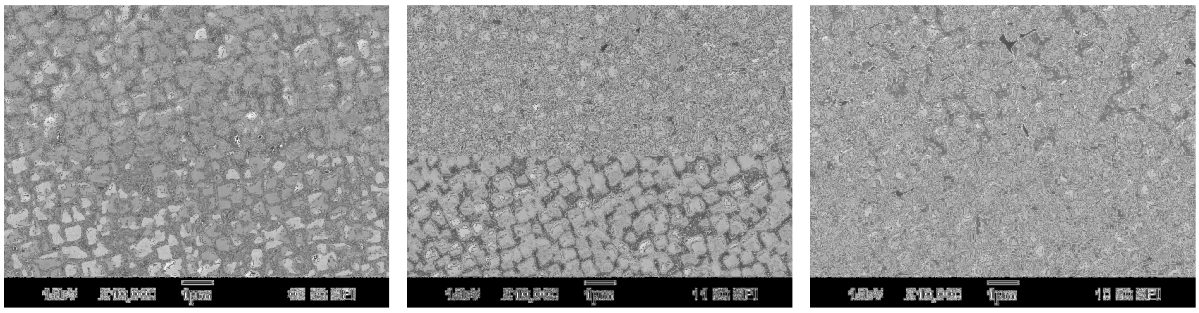

Figure 15: Influence of isothermal heat treatments on microstructures of CM247LC (a) without HT (66 % γ'), (b) 1050°C – 15 min (57 % γ'), (c) TT 1100°C – 15 min (53 % γ')

Consequently, one can assume that temperatures obtained on 2 mm-thick samples were locally higher than 1100°C during induction heating, thereby leading to the dissolution of primary γ' precipitates. Moreover, the precipitation of small secondary γ' precipitates is assumed to have occurred during cooling at -80°C/min cooling rate. For 4 mm-thick samples, the larger thermal dissipation is supposed to have induce local temperature below 1100°C, thus limiting primary γ' dissolution. In the present work, the use of induction heating at temperatures near 1050°C, was not sufficiently precise in terms of applied temperatures, to ensure an homogeneous dissolution of primary γ ' whatever the considered substrate thickness. At such elevated programmed temperatures, especially when a regulation is applied to reduce cooling rate, it becomes difficult to fully control local temperatures with a precision of less than 50°C as shown in Figure 16. However, and this is an interesting point, results tend to confirm that laser cladding can be carried out to refurnish cast CM247LC without inducing hot-cracking, provided local temperatures are increased up to at least 1100°C, and with the use of a controlled cooling rate.

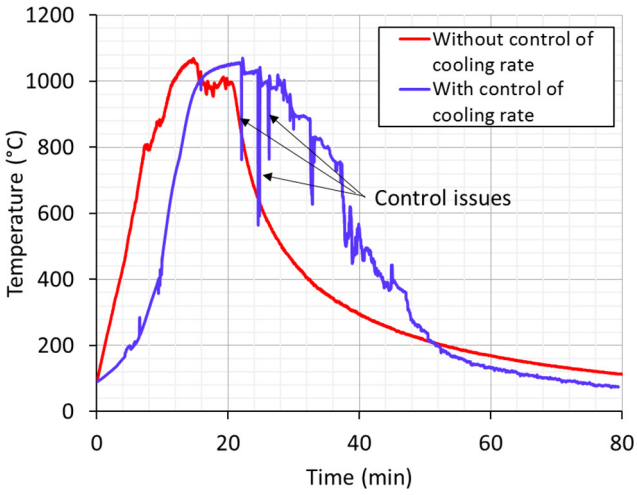

Figure 16*: Examples of thermal cycles generated by the inductor and measured by pyrometer (1050°C programmed temperature) with or without control of the cooling rate (without control : 80°C/min cooling rate, with control : 25°C/min between 1050°C and 750°C). Sharp temperature decreases are evidenced during the inductor heating*

In short, the capability of laser cladding the CM247LC alloy was shown to depend on its local microstructure: for local pre-heating temperature below 1100°C, dissolution of large primary γ' precipitates was not sufficient to avoid hot cracking, whereas a sufficient dissolution was obtained for temperatures at least equal to 1100°C. Such preheating temperatures are rather close from the full γ' dissolution temperature (1230°C). In terms of pre-heating temperature, the current results are in relatively good accordance with arc welding procedures recommended in a patent by Smashey (1999).

5. Summary and conclusions

This work was aimed at defining an experimental protocol for the repairing of CM247LC aeronautic parts having a very high primary γ' content (≈ 65 %). In a first stage, considering single beads, many processing conditions (power, preheating temperature, spot size, scan velocity) have been tested to identify conditions with the least crack sensitivity. Low laser fluence were systematically shown to decrease the crack sensitivity, but no crack-free samples could be obtained for pre-heating conditions of less than 900°C.

In a second stage, considering induction preheating at 1050°C programmed temperature, crack-free welds could be obtained in multi-bead configuration. This was attributed to a huge reduction of primary γ' phase (down to 15 %). Such a result is assumed to be due to local pre-heating temperatures of more than 1100°C. The present work confirmed the ability of laser cladding + induction pre-heating to refurnish cast CM247LC alloy. Further optimization of the induction pre-heating stage should be done to improve the whole process.

In the incoming work, longer induction heating time-maintains, altogether with more temperature measurements should be carried out to ensure a sufficiently precise and stable pre-heating in the 1100-1150°C range. Moreover, after laser repairing with a 1100-1150°C pre-heating, a full range of thermal treatments (stress relief …) should be applied to the repaired material to obtain the desired microstructure and the appropriate mechanical strength.

Acknowledgements

This work was done within the frame of the NENUFAR project granted through the 19th FUI call.

References

(Basak, 2017) Basak, A., Das, S., 2017. Microstructure of nickel-base superalloy MAR-M247 additively manufactured through scanning laser epitaxy (SLE). 2017. J. Alloys Compd. 705, 806–816. doi:10.1016/j.jallcom.2017.02.013

(Carter, 2014) Carter, L.N., Martin, C., Withers, P.J., Attallah, M.M., 2014. The influence of the laser scan strategy on grain structure and cracking behaviour in SLM powder-bed fabricated nickel superalloy. J. Alloys Compd. 615, 338–347. doi:10.1016/j.jallcom.2014.06.172

(Danis, 2010a) Danis, Y., Arvieu, C., Lacoste, E., Larrouy, T., Quenisset, J.-M., 2010a. An investigation on thermal, metallurgical and mechanical states in weld cracking of Inconel 738LC superalloy. Mater. Des. 31, 402–416. doi:10.1016/j.matdes.2009.05.041

(Danis, 2010b) Danis, Y., Lacoste, E., Arvieu, C., 2010b. Numerical modeling of inconel 738LC deposition welding: Prediction of residual stress induced cracking. J. Mater. Process. Technol. 210, 2053–2061. doi:10.1016/j.jmatprotec.2010.07.027

(Ernst, 1987) Ernst, S.C., Baslack III, W.A., Lippold, J.C., 1987. Weldability of High-Strength, Low-Expansion Superalloys.

(Foster, 2001) Foster, M., Updegrove, K., 2001. Welding superalloy articles. US6333484 B1.

(Gharbi, 2013) Gharbi, M., Peyre, P., Gorny, Fabbro, R., C., Carin, M., Caron, D., Morville. S., Le Masson, P., 2013, Influence of various process conditions on surface finishes induced by the direct metal deposition laser technique on a Ti-6Al-4V alloy, *Journal of Materials Processing Tech.* 213, pp. 791-800

(Hagedorn, 2013) Hagedorn, Y.-C., Risse, J., Meiners, W., Pirch, N., Wissenbach, K., Poprawe, R., 2013. Processing of nickel based superalloy MAR M-247 by means of High Temperature - Selective Laser Melting (HT - SLM), in: High Value Manufacturing: Advanced Research in Virtual and Rapid Prototyping. CRC Press, pp. 291–295. doi:10.1201/b15961-54

(Kim, 2011) Kim, I.S., Choi, B.G., Hong, H.U., Yoo, Y.S., Jo, C.Y., 2011. Anomalous deformation behavior and twin formation of Ni-base superalloys at the intermediate temperatures. Mater. Sci. Eng. A 528, 7149–7155. doi:10.1016/j.msea.2011.05.083

(Li, 1997) Li, Z., Gobbi, S.L., Richter, K.H., (1997) Autogenous welding of Hasteloy X to Mar-M247 by laser, Journal of Materials Processing Technology, 70, 285-292

(Lippold, 2011) J.C. Lippold, S.D. Kiser, J.N. DuPont (2011), Welding Metallurgy and Weldability of Nickel-base Alloys, John Wiley & Sons

(Mc Nutt, 2015) McNutt, P.A., 2015. An investigation of cracking in laser metal deposited nickel superalloy CM247LC (d_en). University of Birmingham.

(Morin, 2009) Morin, J. (2009). Weld repair of superalloy materials. US Patent App. 11/497,113.

(Ojo, 2004) Ojo, O.A., Richards, N.L., Chaturvedi, M.C., 2004. Contribution of constitutional liquation of gamma prime precipitate to weld HAZ cracking of cast Inconel 738 superalloy. Scr. Mater. 50, 641–646. doi:10.1016/j.scriptamat.2003.11.025

(Smashey, 1999) Smashey, R.W., Kelly, T.J., Snyder, J.H., Sheranko, R.L., 1999. Welding of nickel-base superalloys having a nil-ductility range. US5897801 A.

(Vitek, 2005) Vitek, J.M., 2005. The effect of welding conditions on stray grain formation in single Single Crystal Welds, Acta Materialia, 53(1), 53-67